Determination of Ballistic Limit for IM7/8552 Using LS-DYNA MAT 261

Alan D. Byar[1], Jenna K. Pang[1], Jeff Iqbal[1] and Jeff Ko[1]
Boeing Research & Technology, Tukwila, WA, 98108

and

Mostafa Rassaian[2]
Boeing Research & Technology, Tukwila, WA, 98108

Abstract

The goal of the NASA ACC High Energy Dynamic Impact Project is to determine the state of the art of dynamic fracture simulations for high velocity impact for composite fuselage shielding applications. Using a building block approach, several computational models considered under NASA ACC are being validated against test data, starting at unconfigured panels and progressing to configured panels under combined out-of-plane and in-plane loading due to ballistic impact. The computational models being evaluated in this project include MAT 162, MAT 213, MAT 261, SPG, and Peridynamics. In this paper, the simulation results using LS-Dyna Material MAT 261 are presented. In particular, a series of blind predictions for unconfigured panels were performed to determine the ballistic limit or V50 velocity. MAT 261 employs failure approach that is generally physically-based using fracture toughness criteria. The overall material model relies on typical ply-level stiffness properties, similar to MAT 162 and other composite continuum damage material models. The fracture toughness values are based on standard tests, and thus are not subject to extensive calibration. This approach is more efficient than performing extensive optimization studies for calibration of parameters. Also, this approach of relying on physical properties reduces the uncertainty of results, as questions concerning the quality and extent of the calibration studies is no longer relevant. However, it was found that carefully controlled coupon-level tests are needed to accurately obtain the required fracture toughness values. Additionally, it should be noted that there is one significant parameter in MAT 261 that does appear to require calibration, and that is the overall failure strain. This is the strain at which the element is deleted, and is not the same as the strain at which damage begins to accumulate. This failure strain is termed EFS (Effective Failure Strain), and is the maximum effective stain for element failure. Simulations have shown that this value will significantly affect impact response and failure. The paper presents the effect of this element failure strain parameter, along with possible uncertainties in fracture toughness values. With an adjusted appropriate value for EFS, it is seen that simulation results compare well with impact test data for predicted penetration velocity.

[1] Structural Analysis Engineer, Structures Technology, 9725 East Marginal Way South, MC 42-56, Tukwila, WA 98108, MC: 42-25, Non-Member.
[2] Technical Fellow, Structures Technology, 9725 East Marginal Way South, Tukwila, WA 98108, MC: 42-56, AIAA Associate Fellow.

I. Introduction

The NASA Advanced Composites Consortium (ACC) seeks to evaluate and transition technology that will support the development and certification of new aircraft structure that utilize advanced composite materials. An overview of the testing and composite model evaluation method is presented in the paper noted in Reference 1, and detailed evaluations of other material modeling approaches are presented in papers noted in References 2-4. The focus of the current work is simulating High Energy Dynamic Impact (HEDI) events. At the present time, a lack of fully validated and standardized analysis approaches has led to the increased use of testing to evaluate the structural response of primary aircraft structure for design and certification. The testing required for HEDI is both expensive and time consuming due to the size, complexity, and wide range of possible design configurations. This paperassesses MAT 261 (*MAT_LAMINATED_FRACTURE_DAIMLER_PINHO) in LS-DYNA for use in predicting the damage response of a composite panel subject to high energy impact. The following sections provide an overview of this material model, a description of the simulation approach for predicting impact response, a presentation of simulation results along with comparisons to test data, and conclusions. The future work will be expended to validated advanced analysis methods for predicting impact damage to large scale configured structures in the Phase 2 of the NASA ACC HEDI project.

II. MAT 261 Overview

LS-DYNA MAT 261 is a continuum damage model that uses physically based failure criteria with linear softening. Failure initiation is stress-based, and damage progression is then determined by fracture toughness for the failure mode which has been activated [5, 6]. As seen in Figure II-1, the softening is linear after reaching failure initiation. MAT 262, which is not considered in this study, allows for bi-linear softening for some failure modes. MAT 262 requires additional fracture toughness parameters, however, and additional testing would be required to establish those values. The failure strain ε^f is a function of both the fracture toughness of the specified mode and the element length. The onset failure strain, ε^0, is determined using stress-based criteria, as frequently seen in composite failure models. The onset failure strain criteria for fiber tensile loading is shown in Figure II-2.

The critical region for predicting damage progression is after the onset failure strain, as this determines the energy dissipated during element loading up to the final erosion limit. There are five damage failure modes included in MAT 261, and each mode requires input for fracture toughness. These five damage modes are:

- Compressive fiber failure
- Tensile fiber failure
- Intra-laminar matrix tensile failure
- Intra-laminar matrix transverse shear failure
- Intra-laminar matrix longitudinal shear failure

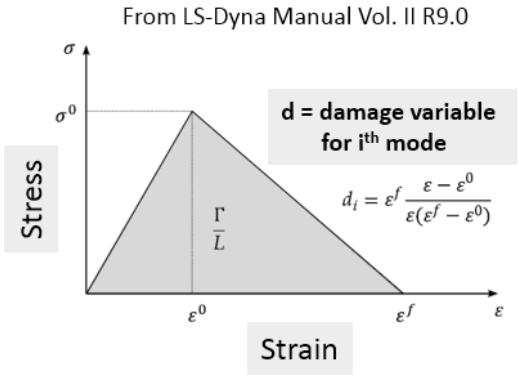

Figure II-1. Use of fracture toughness and element length to determine damage progression

Each of these damage modes requires a fracture toughness value that may be determined from testing. Fiber fracture toughness may be determined using compact compression and compact tension tests. These test coupons are similar, and are used to provide progressive failure and crack growth for both fiber compressive kinking and for tensile failure. Load-displacement data may then be used to calculate fracture toughness. A typical compact tension test simulation is shown below.

Matrix fracture toughness values may be determined from a double cantilevered beam test and 4-point bend test with pre-set crack. The assumptions are that intra-laminar matrix tensile failure is equivalent to Mode I fracture toughness, and that both transverse and longitudinal intra-laminar matrix shear failure is essentially equivalent to Mode II critical fracture toughness. Other tests are

Tensile fiber mode:

$$\phi_{1+} = \frac{\tilde{\sigma}_{11} - \nu_{12}\tilde{\sigma}_{22}}{X_T} \quad \begin{cases} \phi_{1+} > 1 & \text{failure activated} \\ \phi_{1+} \le 1 & \text{no failure} \end{cases}$$

Softening evolution of damage parameter, when failure is activated:

$$d_{1+} = 1 - (1 - d_{1+}^L)(1 - d_{1+}^E)$$

Figure II-2. Stress based failure onset shown for tensile fiber mode failure

also available that could provide these fracture toughness values. For the current study, values were obtained from these four tests for IM7/8552 uni-directional tape.

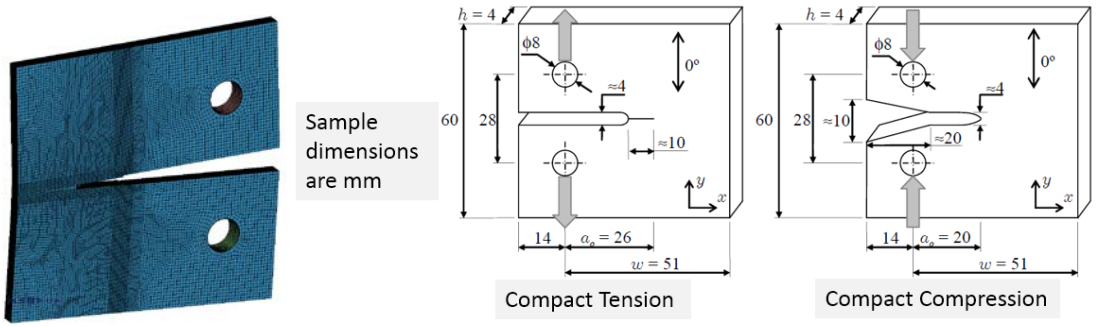

Figure II-3. Compact Tension and Compression Sample Test Configuration and simulation

In addition to fracture toughness, the material model allows for definition of a final erosion strain based on the effective element strain value. This element erosion strain limit has a significant effect of the final impact response, and can influence the impact energy level at which penetration occurs. This is because a higher strain erosion limit allows for additional energy dissipation by the composite element, and lower limits naturally reduce the ability of the element to dissipating impact energy. This effect is seen below in Figure II-4, which was performed on an element level to illustrate the effect. Also, each plot shows results for a range of element sizes in inches, normalized for volume as needed. Results from this plot also show that EFS has a more significant effect on energy dissipation than does element size.

For fiber dominated failure, which has a relatively high fracture toughness value, energy will continue to accumulate as damage progresses. This occurs because the post-onset failure slope is very gradual. In this case, the element erosion strain limit influences the overall amount of energy that is dissipated during impact.

Thus, while MAT 261 is primarily based on physical fracture toughness measurements, it is still necessary to calibrate the EFS valure to provide for reasonable impact response. Even so, this material model still provides a significant advantage over other material models that rely entirely on extensive calibration of artificial damage parameters to simulate post-onset damage progression.

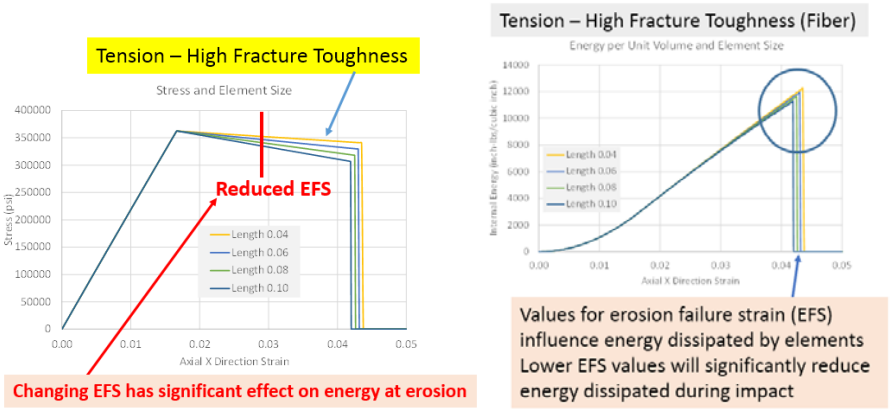

Figure II-4. Effect of Effective Failure Strain (EFS) on element energy dissipation

III. Simulation and Approach

Under Phase I of the NASA ACC HEDI project, ballistic impact testing was performed on flat component-level test articles. Figure III-1 shows a model of one test panel and of two projectiles which were used in testing. An image of the test setup is also shown. The simulations shown in this study were performed with a 40 ply unidirectional tape layup using a traditional laminate. Element discretization was based on an element length of approximately 0.08 inches square for in-plane element lengths in the region of impact. Each ply was modeled with a single element through the thickness. The panel is held in a picture frame support with bolts pre-loaded in accordance with test procedure. Previous simulations have shown that a model which includes a picture frame mounted on load cells provides a nearly equivalent impact response to a model which includes the full frame support, as seen in the test fixture image. The test articles consisted of 25" x 25" panels secured to two square picture-frames and connected to the upright supports through four piezoelectric load cells. The supporting structure behind the load cells is not included in the simulation. The panel material is IM7/8552, and testing was performed as noted above to determine the fracture toughness values for use in the simulation.

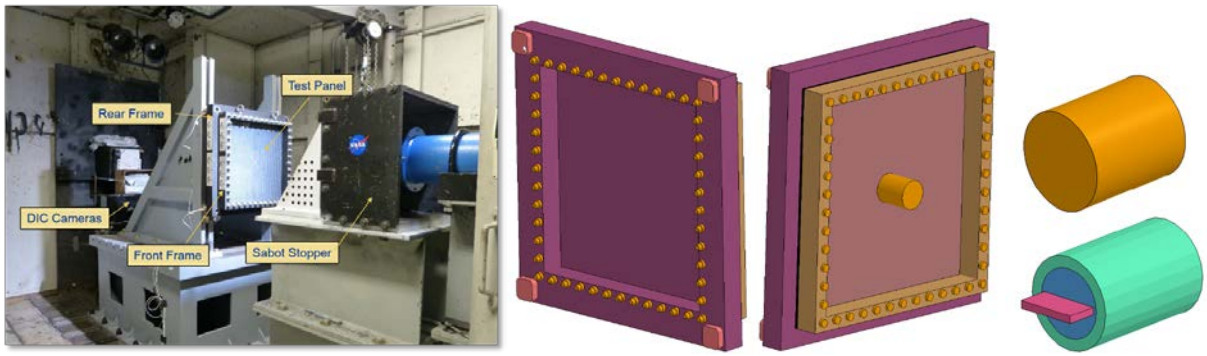

Figure III-1. Test frame and panel, back and front views of model, and blunt and sharp projectiles

Fig. III-2 shows a list of material properties and input parameters for MAT 261 [8]. The five required fracture toughness values are listed, along with several failure options that may be turned on or off. For the simulation, all failure options were activated. This means that fiber tensile failure (DAF), fiber compressive failure (DKF), and matrix shear failure (DMF) were all activated. The model uses cohesive contact type 9 between plies to represent inter-laminar response. Standard testing was performed to determine inter-laminar strength and fracture toughness values. For solid elements, no change in response was observed in simulations where the SOFT parameter was varied. It is possible that the SOFT parameter will effect response for shell elements, which were not considered in this study. A SOFT value of 0.6 was used for all simulations.

		1	2	3	4	5	6	7	8
elastic properties	Card 1	MID	RO	EA	EB	EC	PRBA	PRCA	PRCB
	Card 2	GAB	GBC	GCA	AOPT	DAF	DKF	DMF	EFS
material coordinates	Card 3	XP	YP	ZP	A1	A2	A3		
	Card 4	V1	V2	V3	D1	D2	D3	MANGLE	
material parameters and strength	Card 5	ENKINK	ENA	ENB	ENT	ENL			
	Card 6	XC	XT	YC	YT	SL			
	Card 7	FIO	SIGY	LCSS	BETA	PFL	PUCK	SOFT	

DAF: flag to control failure of an IP based on longitudinal (fiber) tensile failure

DKF: flag to control failure of an IP based on longitudinal (fiber) compressive failure

DMF: flag to control failure of an IP based on transverse (matrix) failure

EFS: Max. effect. Strain for element layer failure. A value of unity would equal 100% strain

ENKINK: Facture toughness for longitudinal (fiber) compressive failure mode

ENA: Facture toughness for longitudinal (fiber) tensile failure mode

ENB: Facture toughness for intralaminar matrix tensile failure

ENT: Fracture toughness for intralaminar matrix transverse shear failure

ENL: Fracture toughness for intralaminar matrix longitudinal shear failure

XC: longitudinal compressive strength

XT: longitudinal tensile strength

YC: transverse compressive strength

YT: transverse tensile strength

SL: longitudinal shear strength

FIO: fracture angle in pure transverse compression (in degrees, default=53.0)

SIGY: In-plane shear yield stress

LCSS: Load curve ID which defines the non-linear in-plane shear-stress as a function of in-plane shear-strain

BETA: hardening parameter for in-plane shear plasticity

PFL: Percentage of layer which must fail before crashfront is initiated.

PUCK: flag to post-process Puck's inter-fiber-failure criterion

SOFT: reduction factor for strength in crashfront elements

Figure III-2. List of input parameters including material properties and user-defined variables

IV. Results and Test-Analysis Comparison

Pre-test predictions with MAT 261 used an Effective Failure Strain value of around 0.045, and consistently under-predicted the ballistic penetration velocity, as seen in subsequent testing. This is shown below in Figure IV-1, which has results for all panels with the blunt projectile. MAT 261 shows similar trends as seen with test, as it predicts lower than expected penetration velocities for both tape and fabric, as well as hybrid tape and fabric panels. For this study, simulations were performed entirely with the 40 ply traditional laminate with unidirection tape. It is assumed that any observations and results from studying this panel response will apply also to the other panels which were tested and simulated.

The V_{50} predictions are low by approximately 30 percent in terms of impact velcocity, indicating that the panel is not dissipating sufficient impact energy in simulation. As shown in Figure II-1 above, energy is dissipated as damage accumulates after onset of initial failure. It was possible that the selected element level effective failure strain (EFS), which determines the element erosion, did not allow for sufficient energy dissipation. An ESF value that is set too low will not allow for sufficient damage progression. A range of effective strain erosion limits was therefore investigated, and it was found that an erosion strain limit of 0.05 led to ballistic limit results that compare well with test data. The results for the adjusted EFS value are also plotted on this figure, showing the change from the pre-test prediction. The updated simulation results show a ballistic limit of around 650 ft/sec, which falls within the range of available test data for the blunt projectile.

Figure IV-2 shows the post-test damage seen in the panel. The simulation damage pattern is seen immediately after penetration, and the composite would likely rebound to a similar shape as seen in testing, if the simulation were run for an extended time period. In the simulation, damaged plies are still bending outward, and have not had time to rebound back toward the panel.

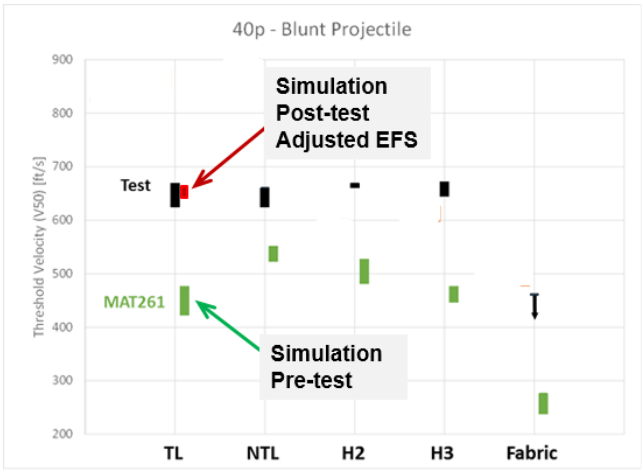

Figure IV-1. Test-analysis – simulation pre-test and simulation with revised EFS

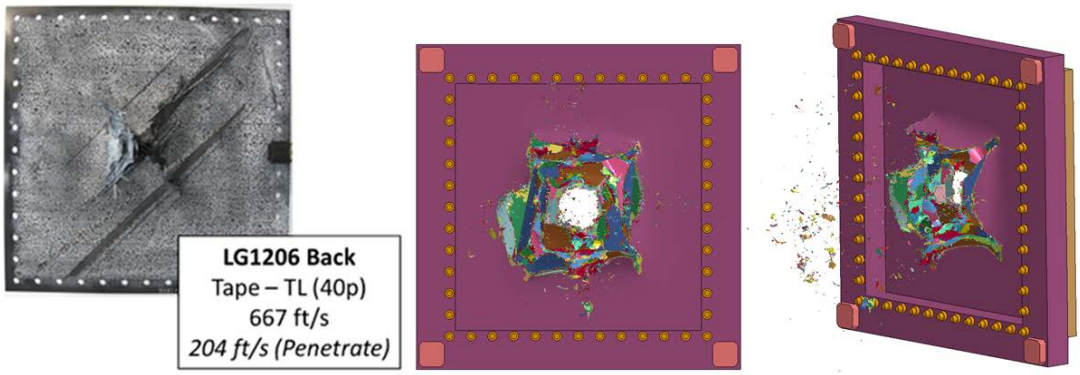

Figure IV-2. Test-analysis comparison of post-test and immediate post-penetration from simulation

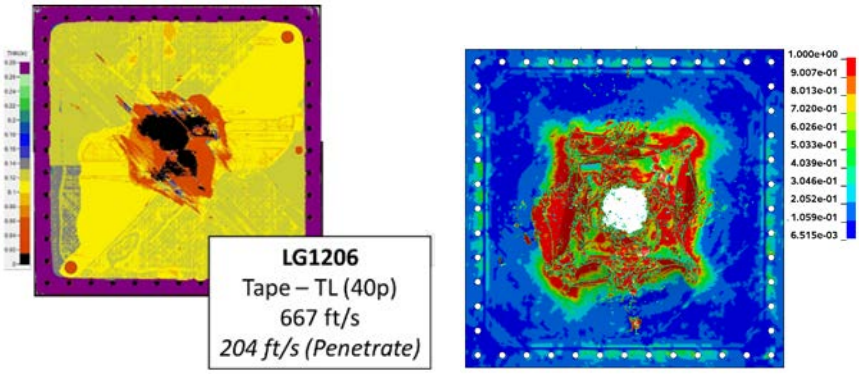

Matrix Damage 1.0 = Failure

Figure IV-3. Test-analysis comparison of NDE from test and matrix failure from simulation

Figure IV-3 Shows a comparison of NDE delamination from test, along with a plot of matrix damage from simulation, which approximates the expected region of delamination.

Figure IV-4 shows full penetration with the blunt projectile at 678 ft/sec, along with damage plots from 628 ft/sec, where the projectile did not penetrate. The damage plot from the back view shows the region of matrix

damage, where 1.0 or over represents complete failure of the matrix. The back view shows the expected region of damage, which is extensive even without penetration of the projectile. These simulations were performed with EFS = 0.05, which is the revised value. The front view at 628 ft/sec shows ply damage and some element erosion, along with significant matrix damage. The damage patterns follow along the top 45 degree ply, as expected. Images of interior plies would show different damage patterns in accordance with the fiber angle.

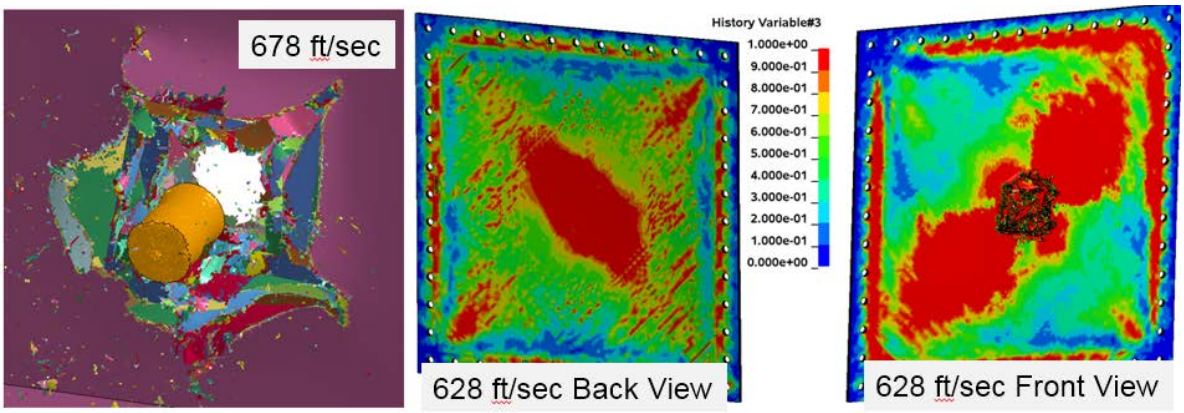

Figure IV-4. Simulation response from 678 ft/sec with penetration and 628 ft/sec with rebound

Simulations were also performed with the sharp projectile, again with the 40 ply tape panel using a traditional laminate. For these cases, it was also necessary to increase EFS in order to compare more reasonably with test data for the ballistic limit. EFS was increased to 0.06, which led to a close correlation between test and simulation responses. For the sharp projectile, rebound and partial damage was found for the simulation case with an initial velocity of 265 ft/sec. Full penetration was found for the simulation case with an initial velocity of 289 ft/sec, which bounds the penetration velocity within a 25 ft/sec range. This V_{50} range compares closely with test data.

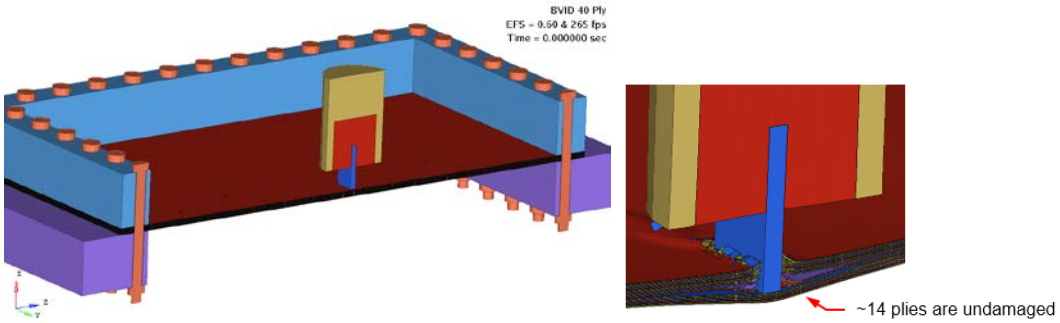

Figure IV-5. Simulation response of sharp projectile at 265 ft/sec – partial pentration - 42 ft/sec rebound velocity, cut view showing half of model

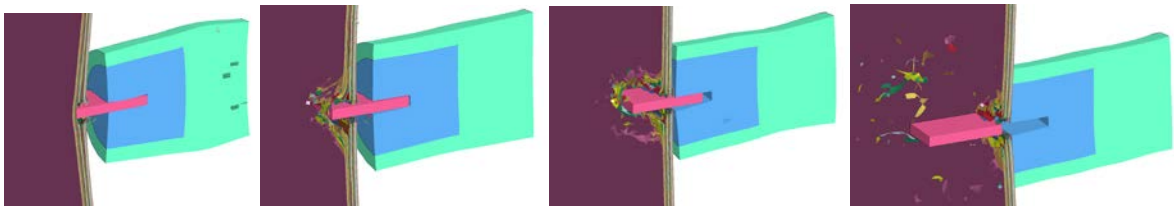

Figure IV-6. Simulation response of sharp projectile showing full penetration with initial velocity of 289 ft/sec, cut view showing half of projectile

Figure IV-5 and Figure IV-6 show panel response to the sharp projectile for two impact cases where there is partial damage and full penetration. At 265 ft/sec, partial penetration occurs, and the blade rebounds. At a slightly

higher impact velocity, 289 ft/sec, full penetration occurs. Matrix and fiber tension damage are shown in Figure IV-7 for the sharp projectile case with an initial velocity of 289 ft/sec. The sharp projectile fully penetrates the panel, but the material encasing the back of the metal blade rebounds, and does not penetrate the panel. Damage to the panel is more closely centered than that seen with the blunt projectile, and matrix failure does not extend to the panel edges. Fiber failure in tension would likely be the dominate failure mode, especially on the back side that is shown in this figure. Fiber failure is grouped closely around the actual point of penetration. As expected, matrix failure extends beyond the region of fiber tension failure, as does matrix damage. These plots were performed using History Variables 1 and 3, and other History Variables are available to interrogate the simulation results with respect to degree of damage for various modes.

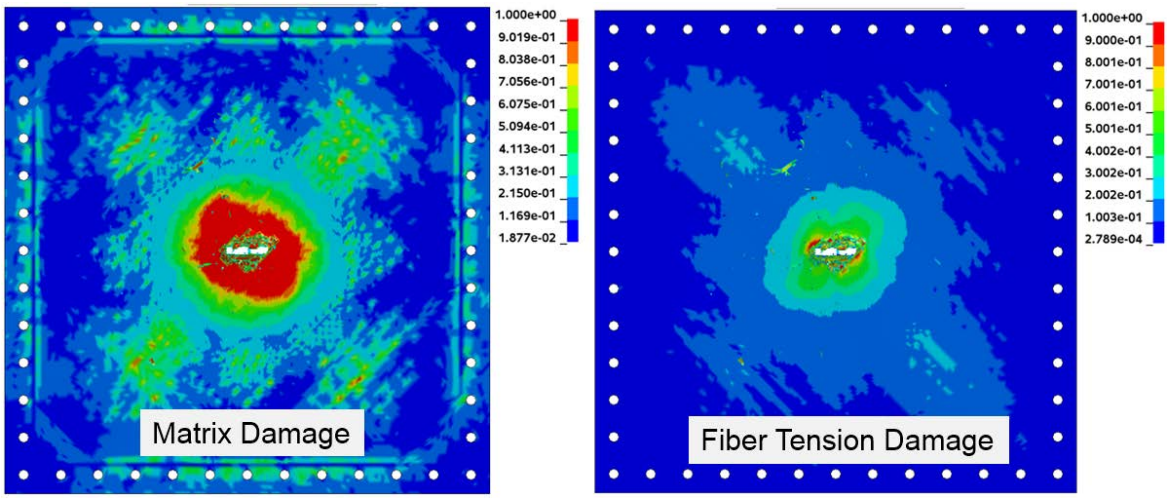

Figure IV-7. Matrix damage and fiber tension damage on 0 to 1.0 scale for sharp projectile at 289 ft/sec, back view after full penetration

The sharp projectile impact simulation was used to study the effect of reducing fiber fracture toughness on impact response. Two simulations were performed in which the fracture toughness was reduced by 20 percent, and it was found that the simulation was not highly sensitive to fiber fracture toughness. This is shown below in Figure IV-8.

Sharp Projectile EFS = 0.40		Sharp Projectile EFS = 0.60	
Initial Velocity (ft/s)	Final Velocity (ft/s)	Initial Velocity (ft/s)	Final Velocity (ft/s)
189	62 - rebound with no penetration	265	69 - rebound with no penetration
189 w/ 20% reduction	54 - rebound with no penetration	265 w/ 20% reduction	23 - rebound with no penetration

Note: 20% reduction in ENKINK & ENA values

Figure IV-8. Effect of reducing fiber fracture toughness – no change in penetration, minor decrease in rebound velocity

The following figure shows a final summary of the adjusted simulation impact response for both sharp and blunt projectiles, as compared with test. All cases are for a 40 ply panel with traditional layup. The Sharp impactor simulation with EFS = 0.06 shows full penetration at 289 ft/sec, with a residual penetration velocity of almost 200 ft/sec. In this simulation, the metal blade separates from the hard rubber cylinder in which it is slotted. Thus the cylinder does not penetrate, and this allows the blade to continue with a relatively high velocity after impact. A reduced impact velocity of 264 ft/sec with the sharp projectile results in partial penetration, as previously shown, with a small rebound velocity.

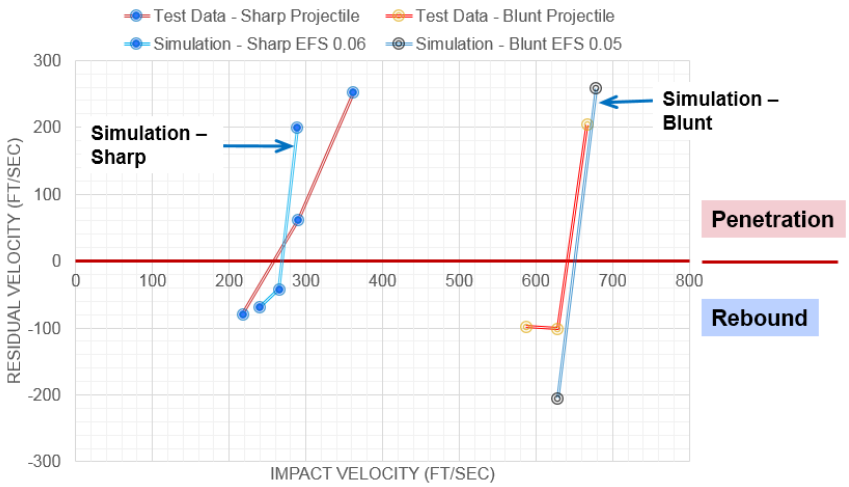

Figure IV-9. Comparison of test and simulation impact response for blunt and sharp projectiles, using adjusted EFS for simulations

For test, we see a similar trend, although the residual penetration velocity for test is somewhat lower than for simulation for a near identical initial impact velocity. A slight increase in the test impact velocity then leads to the expected high residual velocity of the impactor. This case results in approximately 250 ft/sec residual velocity from testing.

The blunt impactor simulation with an EFS of 0.05 compares well with test data, showing a V_{50} of aound 650 ft/sec. This is within the range of V_{50} seen from testing. In simulation, the residual impact penetration is somewhat higher than seen in test, with a velocity of 250 ft/sec from simulation compared with 200 ft/sec from test. The rebound velocity is also higher in simulation than test. It is possible that the material model used for the hard rubber impactor was lacking in fidelity, though the basic properties at point of impact should be reasonable. This means that the residual velocities of the blunt impactor in simulation are not completely reliable. However, the close bracket of penetration to rebound in simulation shows a fairly narrow range for predicted ballistic limit.

The above results show that an appropriate EFS value would be between 0.05 and 0.06 for the cases under consideration. EFS should ideally be treated as a material property, and should not be adjusted on a case-by-case basis. One approach to resolving this would be to choose an EFS value half-way between these two points, meaning that an EFS value of 0.055 could be used for all future simulations with IM7/8552. However, due to the uncertainty involved in representing the blunt projectile, there is higher confidence in the sharp projectile simulations with an EFS of 0.06, and this value should serve as a reasonable baseline for future simulations. More experience with a larger range of impact conditions may lead to further adjustment of this variable.

V. Conclusion

A review and evaluation of LS-DYNA MAT 261 was performed based on prediction of ballistic limits for an IM7/8552 composite panel. This evaluation included an assessment of key input parameters, and a comparison of predicted and test values for V_{50} for 2 different projectiles. Initial pre-test predictions with MAT 261 were below the expected values based on subsequent test data. An increase in the element Effective Failure Strain (EFS) led to very good correlation with test data. While most parameters in MAT 261 are based on physical material properties, EFS requires calibration to ensure that an appropriate element erosion limit is set. This is a known limitation of finite element codes that rely on element deletion to propagate through-thickness cracks.

Specifically, the following findings were made:

1. The value for EFS is the single most important variable for predicting impact damage response. An EFS value of between 0.05 and 0.06 leads to very good correlation with test data for predicting V50 values. With the hard rubber blunt projectile, 0.05 provided the best correlation, and with the sharp metallic projectile, 0.06 provided the best correlation. It should also be noted that there is some uncertainty in characterizing the material properties used in simulating the blunt projectile. For future studies with metallic impactors, a baseline EFS value of 0.06 would appear to be appropriate.
2. For fiber-dominated failure, the simulation shows only minor sensitivity to fiber fracture toughness values. While accurate test data on fiber compression and fiber tensile fracture toughness values is clearly optimal, simulation results show that some uncertainty in these fracture toughness values will not significantly effect predicted penetration response.
3. The fracture toughness values for IM7/8552 which were used in simulation appear to be reasonable in terms of showing appropriate impact and penetration response, when used with the recommended EFS values. EFS works in conjuction with the fracture toughness values to determine the amount of energy dissipated during impact.

Overall, LS-DYNA MAT 261, using baseline physical material properties for IM7/8552, appears to show reasonable predictions for V50 and residual velocity for the impact cases which were studied to date. The predictive capability of MAT 261, using the revised EFS value, will be further evaluated for large scale configured structures under NASA ACC HEDI Phase 2. This work is currently in progress, and new predictive results will determine if the revised EFS value applies to both configured and unconfigured panels.

Acknowledgements

The material in this paper is based upon work supported by NASA under Award No. NNL09AA00A. Any opinions, findings, and conclusions or recommendations expressed in this material are those of the author(s) and do not necessarily reflect the views of the National Aeronautics and Space Administration.

References

1. *NASA ACC High Energy Dynamic Impact Methodology and Outcomes,* by Kenneth J. Hunziker, Jenna K. Pang, Matthew E. Melis, Michael Pereira and Mostafa Rassaian
2. *Dynamic Impact Testing and Model Development in Support of NASA's Advanced Composites Program,* by Matthew E. Melis, Michael Pereira , Robert Goldberg, and Mostafa Rassaian
3. *Comparison of Test Methods to Determine Failure Parameters for MAT162 Calibration,* by Matthew Molitor, Brian Justusson, Jenna K. Pang, and Mostafa Rassaian
4. *Determination of Ballistic Limit for IM7/8552 Using Peridynamics,* by Olaf Weckner, Fernando Cuenca, Stewart Silling, Mostafa Rassaian, and Jenna Pang
5. *Physically-based failure models and criteria for laminated fiber-reinforced composites with emphasis on fiber kinking. Part I: Development,* by S. T. Pinho, L. Iannucci, and P. Robinson, Composites Applied Science and Manufacturing, 2005
6. *Physically based failure models and criteria for laminated fiber-reinforced composites with emphasis on fiber kinking. Part II: FE Implementation,* by S. T. Pinho, L. Iannucci, and P. Robinson, Composites Applied Science and Manufacturing, 2005.
7. *Fracture toughness of the tensile and compressive fiber modes in laminated composites,* by S. T. Pinho, L. Iannucci, and P. Robinson, 2005.
8. *New Material Model for Composites in LS-Dyna*, by Stefan Hartmanm, in Composite Research with LS-DYNA, Stuttgart, 2013.